Title

Stabilizing potentials in bound state analytic continuation methods for electronic resonances in polyatomic molecules

Journal

The Journal of Chemical Physics, 146(4)

ISSN

0021-9606

Authors

White, Alec F

Head-Gordon, Martin

McCurdy, C William

Publication Date

2017-01-28

DOI

10.1063/1.4974761

Peer reviewed

Stabilizing potentials in bound state analytic continuation methods for electronic resonances in polyatomic molecules

Alec F. White,[1,2] Martin Head-Gordon,[1,2,a)] and C. William McCurdy[2,3,b)]
[1)] *Department of Chemistry, University of California, Berkeley, CA 94720 USA*
[2)] *Chemical Sciences Division, Lawrence Berkeley National Laboratory, Berkeley, CA 94720 USA*
[3)] *Department of Chemistry, University of California, Davis, CA 95616 USA*

(Dated: 27 June 2017)

The computation of Siegert energies by analytic continuation of bound state energies has recently been applied to shape resonances in polyatomic molecules by several authors. We critically evaluate a recently proposed analytic continuation method based on low order (type III) Padé approximants as well as an analytic continuation method based on high order (type II) Padé approximants. We compare three classes of stabilizing potentials: Coulomb potentials, Gaussian potentials, and attenuated Coulomb potentials. These methods are applied to a model potential where the correct answer is known exactly and to the $^2\Pi_g$ shape resonance of N_2^- which has been studied extensively by other methods. Both the choice of stabilizing potential and method of analytic continuation prove to be important to the accuracy of the results. We conclude that an attenuated Coulomb potential is the most effective of the three for bound state analytic continuation methods. With the proper potential, such methods show promise for algorithmic determination of the positions and widths of molecular shape resonances.

PACS numbers: 34.80.Bm, 34.20.-b, 32.80.Zb 33.80.Eh

I. INTRODUCTION

Anions that lie energetically above the associated neutral molecule can decay by autodetachment and are therefore characterized by a finite lifetime. Such temporary anions are resonances in the scattering sense and are specified by their energy above that of the neutral molecule, or position,(E_r) and their inverse lifetime or width (Γ).[1–3] These parameters can be specified by a complex Siegert energy

$$E = E_r - i\frac{\Gamma}{2} \tag{1}$$

which specifies the location of the S-matrix pole that is associated with the resonance.[1,4]

Despite their importance in a variety of chemical processes, reliable computation of resonance positions and widths is still far from routine. The primary difficulty arises from the need to consider the electronic continuum. There exists a variety of methods for computing resonance parameters, though none have been sufficiently developed so as to provide a reliable algorithm that can be generally applied even to the low-lying resonances of small molecules. Scattering methods[5–10] treat the continuum with explicit use of scattering boundary conditions in order to compute observables like the cross-section. Stabilization methods[11,12] and associated analytic continuation methods,[13–15] use continuum eigenvalues from bound state calculations to extract resonance parameters. Complex coordinate methods[4,16–21] compute the Siegert energy as an eigenvalue of a transformed, non-Hermitian, Hamiltonian operator. Bound state extrapolation[22,23] or analytic continuation[24,25] methods rely on the analytic continuation of bound-state energies to find resonance parameters. The focus of this study is this final class of methods; in particular, we focus on the method of analytic continuation in the coupling constant (ACCC) for shape resonances in molecules.

The ACCC method was first proposed within the nuclear physics community.[24,26] A potential is added to the Hamiltonian to make the resonance state bound and then the bound state energies are analytically continued, as a function of the potential coupling, to determine the Seigert energy at zero coupling. Nestmann *et al.*[22,23] independently proposed an extrapolation method for molecular resonances based on scaled nuclear charges. Recently, these two methods have been combined and applied to molecular shape resonances.[25,27–30] In most of these studies, a Coulomb potential is used to bind the resonance as in the method of scaled nuclear charges. The exception is the manifestly short-range Voronoi potential suggested by Sommerfeld *et al.*[28] Sommerfeld and coworkers noted that the long-range Coulomb potential is not formally applicable and obtained much more consistent results with their Voronoi potential. Despite this fact, methods employing a Coulomb potential have had moderate success with shape resonances in polyatomic molecules. However, these methods suffer from two well-understood afflictions. The first is associated with the difficulty in representing the analytic structure of the resonance trajectory which, for short-range potentials, has a square root branch point in the complex momentum plane.[1,3] The second is that the analytic continuation it-

[a)] Electronic mail: mhg@cchem.berkeley.edu
[b)] Electronic mail: cwmccurdy@ucdavis.edu

self can easily become numerically unstable.[31,32]

Horáček and coworkers have made a recent attempt to ameliorate these issues.[29,30] Their method, which they have termed regularized analytic continuation (RAC), relies on the inverse variant of the ACCC method (IACCC) and therefore avoids many of the difficulties associated with the analytic structure of the resonance in the complex-momentum plane. Furthermore, they have incorporated the known features of the analytic structure of the problem into low order Padé approximants which are well-behaved numerically. Unfortunately, the functional form of the RAC Padé approximants is formally appropriate only for short-range potentials and not for the Coulomb potentials with which it has been applied.

In this study we evaluate the RAC method of Horáček and coworkers and compare their low order, type III Padé approximants with a high-order, type II Padé approximant for the analytic continuation of the inverse problem. Both functional forms are used along with three classes of potential: a Coulomb potential that is consistent with previous work, a Gaussian potential, and an attenuated Coulomb potential. The Gaussian and attenuated Coulomb potentials are short-range and therefore compliant with the formal requirements of the ACCC method. These methods are applied to two problems where the answer is largely known: a model diatomic potential which is numerically solvable, and the $^2\Pi_g$ shape resonance in $e-N_2^-$ scattering.

II. THEORY

The methods discussed in this paper are based on the IACCC method. In the ACCC method, the Hamiltonian is modified by the introduction of an attractive potential and expressed as a function of a coupling constant λ:

$$H(\lambda) = H + \lambda U. \tag{2}$$

The energy of the desired state is then evaluated at several values of λ that are large enough that the desired state is bound. In other words, the energy of the anion relative to the neutral molecule, E, is negative. Introducing a momentum-like variable, κ, such that $E \equiv -\kappa^2$ we construct an analytic continuation $\kappa(\lambda)$. Finally, κ is evaluated at $\lambda = 0$ to obtain the complex Siegert energy associated with the resonance.

Unfortunately, even in the case where U is short-range (falling off at large distances faster than $1/r^2$), the analytic structure of the momentum is such that it has a square root branch point which must be properly represented as a function of λ. A simpler and numerically better behaved method is the analytic continuation of the inverse problem (IACCC).[29,33] In this method the procedure is the same except that starting from a set of computed values of κ for corresponding values of λ, we construct $\lambda(\kappa)$ and find its zeros to determine the Siegert energy.

$\lambda(\kappa)$ is constructed using a Padé approximant.[32] The method of determining the fit from the input points is important to the results, and finite order Padé approximants are in usually constructed in one of three ways. Type I Padé approximants are determined by matching the coefficients of a power series about a single point. This method is not applicable to the IACCC method as applied here. Type II Padé approximants are required to interpolate some set of input points. Type III Padé approximants are determined by minimizing the χ^2 error in the fit.

A. The type III (RAC) method

The regularized analytic continuation (RAC) method of Horáček and coworkers specifically relies on low order, type III Padé approximants to accomplish the analytic continuation of $\lambda(\kappa)$. The low order Padé approximants recommended in Ref. 29 have functional forms given by

$$\lambda^{[2/1]}(\kappa) = \lambda_0 \frac{\kappa^2 + 2\alpha^2\kappa + \alpha^4 + \beta^2}{\alpha^4 + \beta^2 + 2\alpha^2\kappa} \tag{3}$$

$$\lambda^{[3/1]}(\kappa) = \lambda_0 \frac{(\kappa^2 + 2\alpha^2\kappa + \alpha^4 + \beta^2)(1 + \delta^2\kappa)}{\alpha^4 + \beta^2 + \kappa[2\alpha^2 + \delta^2(\alpha^4 + \beta^2)]} \tag{4}$$

$$\lambda^{[4/2]}(\kappa) = \lambda_0 \frac{(\kappa^2 + 2\alpha^2\kappa + \alpha^4 + \beta^2)(\kappa^2 + 2\gamma^2\kappa + \gamma^4 + \delta^2)}{(\alpha^4 + \beta^2)(\gamma^4 + \delta^2)(1 + \mu^2\kappa)(1 + \mu^2\epsilon^2\kappa)} \tag{5}$$

where

$$\mu^2 = \frac{2}{\epsilon^2 + 1}\left[\frac{\alpha^2}{\alpha^4 + \beta^2} + \frac{\gamma^2}{\gamma^4 + \delta^2}\right]. \tag{6}$$

These functional forms are specifically constructed to conform to the known analytic structure of $\lambda(\kappa)$ in that the square root branch cut requires that $\lambda(\kappa) \sim \lambda_0 + b\kappa^2$ as $\kappa \to 0$. In Ref. 30 a slightly different [4/2] Padé approximant is suggested, but we will not investigate this alternate functional form in this study. The optimal least-squares fit is obtained by solving the non-linear optimization problem. In the present study, this problem is solved using Newton's method with analytic first derivatives and finite difference second derivatives. The expressions for the first derivatives of these expressions are given in Appendix A.

B. The type II method

We have also investigated the use of high order Padé approximations for analytic continuation of $\lambda(\kappa)$. While the use of high order Padé approximants for analytic continuation has known numerical problems,[31] we are unaware of applications of this particular method to the inverse problem.

We use the continued fraction representation given by Schlessinger:[34]

$$\lambda(\kappa) = \frac{\lambda(\kappa_1)}{1+}\frac{a_1(\kappa-\kappa_1)}{1+}\cdots\frac{a_n(\kappa-\kappa_n)}{1}. \tag{7}$$

For n input points, this yields a $[N/M]$ Padé approximant where $N+M=n$ and

$$M = \begin{cases} N & , n \text{ even} \\ N-1 & , n \text{ odd} \end{cases}. \tag{8}$$

This is sometimes called a type II, or Thiele-type, Padé approximant. This representation has the advantages that it exactly interpolates all of the input points and does not require the solution a non-linear least squares problem. However, due to the more complicated form, the zeroes must be found numerically. We use Newton's method to solve the root search problem.

C. The added attractive potential

The precise form of the attractive potential U is flexible, though it must be short range: it must decay faster than r^{-2} at large distances if the analytic structure of $\kappa(\lambda)$ is to be a square root branch point at the critical value of λ where the resonance becomes bound. Despite this restriction, many other authors have advocated using a Coulomb potential. This functional form has the advantage that it requires little to no modification of existing quantum chemistry software, but it is not short-range. The given justification is that in a finite basis, the low-energy part of the spectrum can be effectively ignored so that the long-range part of the Coulomb potential is not important. While it may be effective in practice, this argument lacks formal justification. We will therefore consider two types of added potentials.

First, we consider a Coulomb potential of the form:

$$U_C(\mathbf{r}) = -\lambda\sum_A \frac{Z_A}{|\mathbf{r}-\mathbf{R}_A|}. \tag{9}$$

This differs slightly from the potential used in Ref. 29 but is identical to the potential used in other studies.[22,23,28]

Second we consider an attractive Gaussian potential of the form

$$U_G(\mathbf{r}) = -\lambda\sum_A Z_A e^{-\alpha(\mathbf{r}-\mathbf{R}_A)^2}. \tag{10}$$

This potential is chosen to transform as the totally symmetric representation of the molecular point group. The proportionality to the nuclear charges is chosen in analogy with U_C to provide a potential which will affect molecular many-electron states in a balanced way. Note that α is a free parameter that can be chosen arbitrarily in theory, though it will turn out to be important in practice. The appropriate integrals required for matrix elements of such a potential are 3-center overlap integrals and are easily computed by a variety of methods. We briefly describe the computation of such integrals in Appendix B.

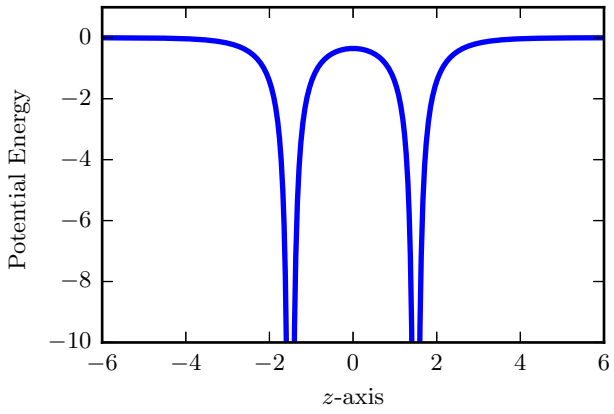

FIG. 1. The model potential given in Equation 12 is plotted along the line defined by the two nuclei. We take this line to be the z-axis.

Finally, we consider an attenuated-Coulomb potential of the form:

$$U_{AC}(\mathbf{r}) = -\lambda\sum_A \frac{Z_A \mathrm{erfc}\left(\omega|\mathbf{r}-\mathbf{R}_A|\right)}{|\mathbf{r}-\mathbf{R}_A|}. \tag{11}$$

Unlike the Coulomb potential, this potential is short-range. In contrast to the, also short-range, Voronoi potential of Sommerfeld and Ehara,[28] the molecular integrals over this potential are similar to those required for certain attenuated electronic structure methods and are therefore available in many quantum chemistry programs.[35,36] ω is likewise a free parameter.

III. RESULTS FOR A MODEL POTENTIAL

In order to test these methods on a problem where the answer is known to high numerical accuracy, we can construct a model 1-electron potential that approximates an effective diatomic molecular potential from electron-molecule scattering. We will use $\mathbf{A}$ and $\mathbf{B}$ to denote the centers of the two "nuclei." The model potential is of the form

$$V(\mathbf{r}) = -e^{-1.5r_A}\left(\frac{1}{r_A}+1\right) - e^{-1.5r_B}\left(\frac{1}{r_B}+1\right) \tag{12}$$

where

$$r_A = |\mathbf{r}-\mathbf{A}| \qquad r_B = |\mathbf{r}-\mathbf{B}|. \tag{13}$$

A plot of this potential along the line defined by the positions of the two nuclei is shown in Figure 1. There is, to our knowledge, no analytical solution to this problem, but the problem has cylindrical symmetry and may

be solved numerically in prolate-spheroidal coordinates using grid methods. This potential supports a bound σ_g-like state ($m = 0$, symmetric under inversion), and a σ_u-like state ($m = 0$, anti-symmetric under inversion) which is a bound state at large (> 4) internuclear distances and a resonance at short internuclear distances. For the purpose of this investigation, we want the second state to be a resonance, so we set the "internuclear" distance to $|\mathbf{A} - \mathbf{B}| = 3$.

A. Numerical details

In order to perform the analytic continuation methods described in the introduction we add either a Coulomb potential of the form

$$U_C(\mathbf{r}) = -\lambda \left(\frac{1}{r_A} + \frac{1}{r_B} \right), \tag{14}$$

a Gaussian potential of the form

$$U_G(\mathbf{r}) = -\lambda \left(e^{-\alpha r_A^2} + e^{-\alpha r_B^2} \right), \tag{15}$$

or a screened Coulomb potential of the form

$$U_{GC}(\mathbf{r}) = -\lambda e^{-\alpha (r_A + r_B)^2} \left(\frac{1}{r_A} + \frac{1}{r_B} \right). \tag{16}$$

The Gaussian-attenuated Coulomb potential is similar to the erfc-attenuated Coulomb potential that we have used for molecular calculations. All three have cylindrical symmetry and are easily representable in prolate spheroidal coordinates.

Schrödinger's equation was solved in prolate-spheroidal discrete variable representation (DVR) basis for $m = 0$. The DVR method is described in detail in Refs. 37–39. We used 15 points in the η variable and 200 points on the interval (0, 100) in ξ. All eigenvalues used for analytic continuation were converged to better than 10 significant figures and 10 significant figures were used in all analytic continuations.

The resonance energy was computed by complex scaling the ξ variable as described in Ref. 37. At this internuclear distance ($R_{AB} = 3$), the resonance has a position of 0.02555645961 and a width of 0.02354423918 in units natural to the problem. These values are similar to those of the σ_u-shape resonance in e^--H_2 scattering, in atomic units, at a slightly stretched geometry.

B. Evaluation of analytic continuation methods

The analytic continuations were each accomplished from 15 bound state energies bound by 0.01-0.3 units of energy. This is roughly based on the recommendations given in Ref. 29. The resonance position and width were computed with type II ([8/7] in this case), type III [2/1], and type III [4/2] methods. The three classes of stabilizing potentials are Coulomb potentials (Equation 14), Gaussian potentials (Equation 15), and Gaussian-attenuated Coulomb potentials (Equation 16). We furthermore tested Gaussian potentials with three different exponents, $\alpha = 0.01, 0.1, 1.0$, and Gaussian-attenuated Coulomb potentials with exponents of $\alpha = 0.005, 0.025, 0.25$.

The results are shown in Table I along with percent error relative to the numerically exact answer. For this model system, the type II method almost universally outperforms the type III methods by a significant margin. In particular, the widths computed by the type III methods are significantly smaller than the true widths. The type II method is significantly more accurate, but still has relative errors on the order of a couple of percent in some cases which, while small compared to those of the type III methods, are large compared with the accuracy of the input values. We attribute the large errors in the type III methods to be due to insufficient flexibility in the functional form used to fit $\lambda(\kappa)$. On the other hand, the errors in the type II method could be partially due to the inherent numerical instability of extrapolation using high order Padé approximations. This is supported by the fact that the error in the type II calculations is of indeterminate sign. For the type III calculations, the width is always underestimated which suggests some systematic error. We shall see that in real molecular calculations, where the width is often significantly smaller than the position, the type III method may not so drastically underestimate the width.

The type III [4/2] Padé approximant improves very slightly over the results obtained with a [2/1] Padé approximant, but at the cost of a much more difficult nonlinear optimization.

Across all analytic continuation schemes the Gaussian-attenuated Coulomb potential produces the most accurate results. The results with the Gaussian-attenuated Coulomb potentials are slightly better than those obtained with a Coulomb potential and significantly better than those obtained with the various Gaussian potentials. Note that the Gausian-attenuated Coulomb potential with the smallest attenuation parameter produces the best results across all methods. This is not surprising, since the theory should be ideal for short-range potentials. However, it is surprising that the that long-range Coulomb potential produces such accurate results compared with the short-range Gaussian-potentials.

Since the attenuated Coulomb potential must ultimately reproduce the results of the Coulomb potential as $\alpha \to 0$, we expect the optimal value of α to be small enough that the potential is minimally distorted in the valence region, but large enough that the potential is still effectively short-range. This "optimal α" will depend on the basis set. For this model problem, our basis extends to $\xi = 100$, and the results in Table I (c) indicate that the optimal α is less than or equal to $\alpha = 0.005$.

		Type II		Type III [2/1]		Type III [4/2]	
		Position	Width	Position	Width	Position	Width
	Coulomb	0.025644	0.023308	0.027575	0.009680	0.023961	0.012078
	Gaussian ($\alpha = 0.01$)	0.025839	0.022663	0.027013	0.001845	0.023024	0.004761
	Gaussian ($\alpha = 0.1$)	0.025681	0.024694	0.026386	0.003606	0.018890	0.017603
(a)	Gaussian ($\alpha = 1.0$)	0.024454	0.021806	0.026375	0.002578	0.021244	0.006470
	Gauss. Coul. ($\alpha = 0.005$)	0.025561	0.023651	0.030915	0.016863	0.027157	0.019401
	Gauss. Coul. ($\alpha = 0.025$)	0.025448	0.023504	0.028691	0.010971	0.025458	0.013786
	Gauss. Coul. ($\alpha = 0.25$)	0.025731	0.023798	0.027957	0.009963	0.024448	0.012618
	Coulomb	0.343	-1.005	7.898	-58.884	-6.244	-48.699
	Gaussian ($\alpha = 0.01$)	1.106	-3.745	5.701	-92.165	-9.908	-79.778
	Gaussian ($\alpha = 0.1$)	0.487	4.883	3.245	-84.685	-26.086	-25.233
(b)	Gaussian ($\alpha = 1.0$)	-4.314	-7.383	3.204	-89.049	-16.873	-72.520
	Gauss. Coul. ($\alpha = 0.005$)	0.017	0.453	20.968	-28.376	6.263	-17.599
	Gauss. Coul. ($\alpha = 0.025$)	-0.426	-0.171	12.267	-53.403	-0.384	-41.445
	Gauss. Coul. ($\alpha = 0.25$)	0.682	1.077	9.394	-57.683	-4.337	-46.408
	Coulomb	0.523		25.659		21.149	
	Gaussian ($\alpha = 0.01$)	1.861		38.906		34.569	
	Gaussian ($\alpha = 0.1$)	2.090		35.553		25.939	
(c)	Gaussian ($\alpha = 1.0$)	4.989		37.370		33.992	
	Gauss. Coul. ($\alpha = 0.005$)	0.190		22.442		9.304	
	Gauss. Coul. ($\alpha = 0.025$)	0.393		24.967		17.343	
	Gauss. Coul. ($\alpha = 0.25$)	0.766		25.597		19.812	

TABLE I. Positions and widths, percent relative error (signed) in positions and widths, and percent relative error of the complex resonance energy are shown in panels a, b, and c respectively. All values are computed for the model problem using the specified stabilizing potential with the given analytic continuation method. Compare with the numerically exact value– Position: 0.02555645961, Width: 0.02354423918.

C. Analytic structure of the resonance trajectory

In order to further evaluate the analytic continuation methods described in this study, we investigate the behavior of the resonance pole under the influence of an added Gaussian, Coulomb, or Gaussian-attenuated Coulomb potential. The trajectory of the resonance as it becomes bound under the influence of a Gaussian potential ($\alpha = 0.1$) is shown in Figure 2. This behavior is well-understood,[1] and it is therefore somewhat surprising that the type III method is not successful with this potential since it precisely encodes the correct analytic structure. However, though the type III methods have the correct form of $\lambda(\kappa)$ near $\kappa = 0$, it is possible that the small number of free parameters are not sufficient to adequately model the function away from $\kappa = 0$. Note that in Figure 2, the behavior of the resonance far away from $\kappa = 0$ is complicated and likely not well modeled by the simple functional forms used in the type III method.

The trajectory of the resonance as it becomes bound under the influence of a Coulomb potential is shown in Figure 3. Note that the resonance crosses $E = 0$ with a finite, negative imaginary part. This behavior, which plays a role in theories of dissociative recombination,[40] has been known for quite some time,[41–43] and it was also recognized in Ref. 44, where it was further shown that the pole corresponding to the resonance is not analytically connected to that of the bound state. It is evident from Figure 3 and from Ref. 44 that the analytic structure that is built into the RAC class of type III approximations is not correct for a Coulomb potential: the resonance does not even pass through the point $E = -\kappa^2 = 0$ in the energy plane.

However, in contrast to the case of a Gaussian potential, the behavior of the resonance far from $\kappa = 0$ is quite simple: the large linear region in energy space gives rise to a large square-root region in momentum space. In this sense, the Coulomb potential appears to be ideal for the type III methods except for near $\kappa = 0$.

The trajectory of the resonance as it becomes bound under the influence of the Gaussian-attenuated Coulomb potential ($\alpha = 0.025$) is shown in Figure 4. The Gaussian-attenuated coulomb potential is short-range, and, as with the Gaussian potential, this fact is reflected in the behavior at the origin. However, the behavior away from the origin is more similar to that of the Coulomb potential: there is a large linear region in energy space. The Gaussian-attenuated Coulomb potential retains the desirable features of the Coulomb potential while still being short-range.

IV. RESULTS FOR THE N_2^- SHAPE RESONANCE

All calculations were performed on N_2^- at its equilibrium geometry (N≡N = 1.094Å). A slightly modified version of the Q-Chem 4 quantum chemistry package[45] was used for all computations. This problem has been very

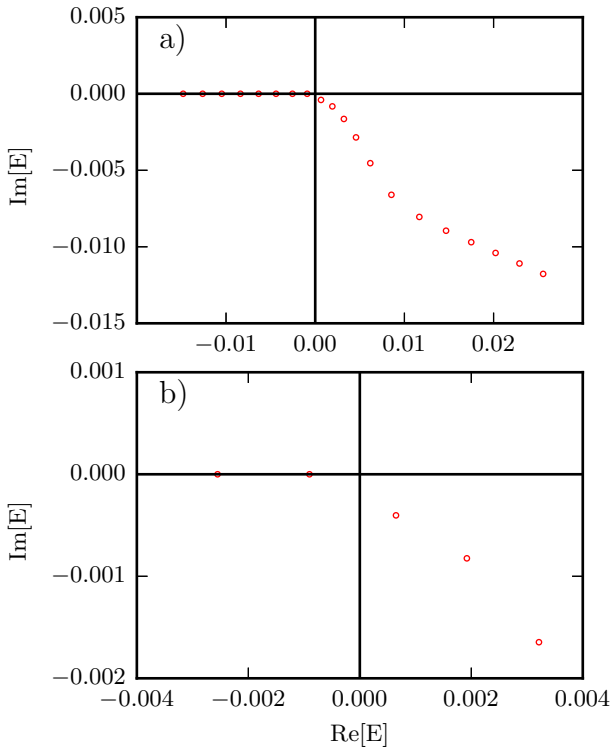

FIG. 2. The behavior of the resonance under the influence of an attractive Gaussian ($\alpha = 0.1$) potential is shown in (a) with a detailed view near the origin in (b). The coupling constant is increased in the range $\lambda = 0.00, \ldots, 0.038$. At $\lambda = 0$ the resonance is at the lower right of (a). As the potential increases, the resonance's position and width decrease until it becomes bound when passing through $E = 0$.

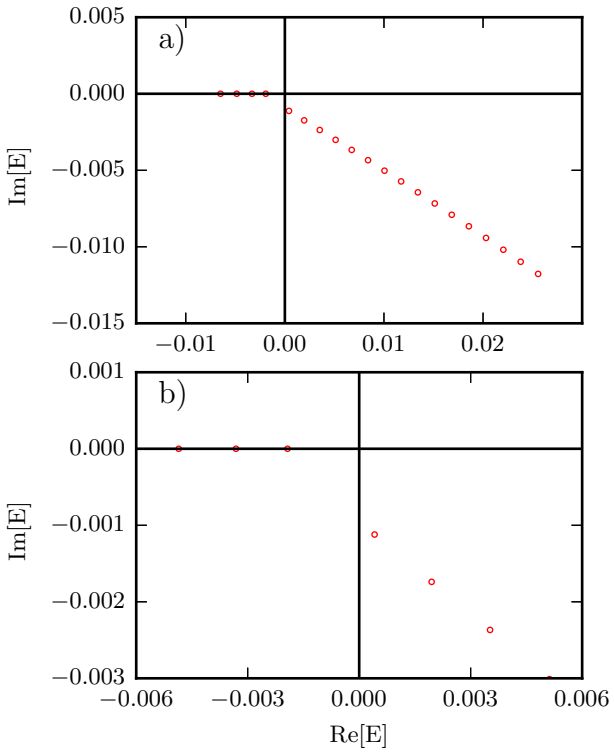

FIG. 3. The behavior of the resonance under the influence of an attractive Coulomb potential is shown in (a) with a detailed view near the origin in (b). The coupling constant is increased in the range $\lambda = 0.00, \ldots, 0.038$. At $\lambda = 0$ the resonance is at the lower right of (a). As the potential increases, the resonance's position and width decrease, but it does not pass through $E = 0$. The point $\lambda = 0.032$ is omitted because the limits of complex scaling prevent us from easily distinguishing the resonance.

thoroughly studied, and some selected literature values are shown in Table II. The experimental estimate given in Ref. 52 is nearly unique in the electron-molecule scattering literature in that it is an estimate of the position and width of the pure *electronic* resonance and therefore directly comparable to the results of our computations. We will refer to this experimentally derived estimate ($E_r = 2.32$ eV, $\Gamma = 0.41$ eV) as the accepted value.

We compare results at the ΔSCF and ΔCCSD(T) levels of theory. Further results at intermediate levels of theory (ΔMP2, ΔCCSD) are shown in the supporting material and in selected cases. We use the correlation-consistent basis sets of Dunning and coworkers.[53,54] The double and triple augmenting functions were obtained by even-tempered extrapolation. For a given basis and angular momentum, the even-tempered factor was taken to be the ratio between the exponents of the most diffuse valence basis function and the augmenting function as specified in the appropriate aug-cc-pVXZ basis set.

In all cases a minimum of 20 (maximum of 23) different coupling strengths corresponding to electron affinities in the range 0 - 20 eV were used in the analytic continuation. This corresponds to type II Padé approximants with a minimum order of [10/10] and maximum order of [12/11].

A. Evaluation of the type III-Coulomb method

The results of the type III method using an attractive Coulomb potential for the N_2^- shape resonance are shown in Table III. We will focus on the [2/1] Padé approximant. However, for completeness, we show some results obtained with a [4/2] Padé approximant.

The [2/1] Padé approximation proved to be simple to implement and we found the least squares problem to be easily solved. Furthermore, the method appears to be numerically stable and the computed resonance parameters converge well with respect to basis set size. Comparing with the literature values in Table II we see that positions computed with the type III-Coulomb method agree modestly with the large spread of different theoretical values. But more importantly, the computed position seems to converge well to the experimental estimate of the position in a large basis set at the ΔCCSD(T) level of theory. However, the width computed with the type III-Coulomb method is consistently too large, and does not converge to the correct limit with increasing basis set size and level of theory. The performance of the type III method on

method	position	width
Stieltjes imaging[46]	2.23	0.40
Schwinger variational + ADC(3) optical potential[47]	2.534	0.536
3rd order decouplings of dilated electron propogator[48]	2.11	0.18
EOM-EA-CCSD stabilization (aug-cc-pV5Z)[49]	2.49	0.5
CAP EOM-EA-CCSD (1st order, aug-cc-pVQZ + 3s3p3d)[50]	2.478	0.286
NH-ROHF with complex basis functions[51]	2.95	0.31
NH-UHF with complex basis functions[51]	2.83	0.22
Experimental estimate[52]	2.32	0.41

TABLE II. Selected literature values (in eV) for the resonances studied here from experiment and various levels of theory. The experimental estimate given in the final line is an estimate of the purely electronic resonance parameters that has been extracted from experiment.

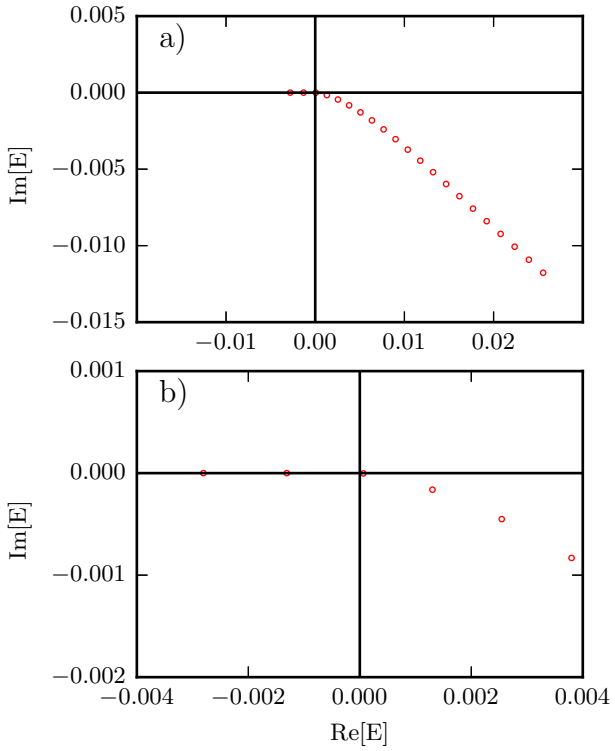

FIG. 4. The behavior of the resonance under the influence of an attractive Gaussian-attenuated Coulomb potential is shown in (a) with a detailed view near the origin in (b). The coupling constant is increased in the range $\lambda = 0.00, \ldots, 0.040$. At $\lambda = 0$ the resonance is at the lower right of (a). As the potential increases, the resonance's position and width decrease. The complex energy passes through the origin at approximately $\lambda \approx 0.036$.

method	basis	Position	Width
ΔSCF [2/1]	aug-cc-pVDZ	2.74110	0.70651
	d-aug-cc-pVDZ	2.73775	0.70488
	t-aug-cc-pVDZ	2.73815	0.70516
	aug-cc-pVTZ	2.76426	0.62306
	d-aug-cc-pVTZ	2.76112	0.62566
	t-aug-cc-pVTZ	2.76130	0.62669
	aug-cc-pVQZ	2.76009	0.62897
	d-aug-cc-pVQZ	2.75868	0.62994
	t-aug-cc-pVQZ	2.75874	0.63018
ΔCCSD(T) [2/1]	aug-cc-pVDZ	2.55676	0.76962
	d-aug-cc-pVDZ	2.49716	0.77837
	t-aug-cc-pVDZ	2.51582	0.77359
	aug-cc-pVTZ	2.41758	0.61607
	d-aug-cc-pVTZ	2.37994	0.62489
	t-aug-cc-pVTZ	2.37848	0.62606
	aug-cc-pVQZ	2.35872	0.60604
	d-aug-cc-pVQZ	2.33451	0.61071
	t-aug-cc-pVQZ	2.33383	0.61100
ΔCCSD(T) [4/2]	t-aug-cc-pVQZ	2.3658	0.5531

TABLE III. Positions and widths (in eV) of the $^2\Pi_g$, N_2^- shape resonance computed using the type III-Coulomb method. Note the favorable convergence with respect to basis set size.

this particular problem is better than might be expected from the application to the model potential. This may be because, unlike in the case of the model potential, the width is almost an order of magnitude smaller than the position. This could reduce the error due to behavior of the resonance near $\kappa = 0$.

The use of a [4/2] Padé approximant (also see supplementary material: Table II) does not significantly change the computed positions and widths. However, we found the least squares problem to be significantly more difficult to solve and in some cases complicated by multiple solutions. It is possible that the [4/2] Padé approximant suggested in Ref. 30 will give better results. We also used a [3/1] Padé approximate, but, in comparison with the [2/1] Padé approximant, we found the differences in both the practical aspects and the results to be insignificant.

B. Evaluation of the type II-Coulomb method

The results for the type II-Coulomb method are shown in Table IV. As expected, the width appears to be slightly more accurate than that computed with the type III-Coulomb method, but it is more difficult to converge the results with respect to the basis set size. The type II method proved to be simple to use, and in no case did

method	basis	Position	Width
ΔSCF	aug-cc-pVDZ	2.8326	-0.0029
	d-aug-cc-pVDZ	2.8096	0.2590
	t-aug-cc-pVDZ	2.8462	0.1863
	aug-cc-pVTZ	2.8003	0.0051
	d-aug-cc-pVTZ	2.8324	0.1629
	t-aug-cc-pVTZ	2.7967	0.1955
	aug-cc-pVQZ	2.8124	0.1138
	d-aug-cc-pVQZ	2.8175	0.2344
	t-aug-cc-pVQZ	2.8206	0.2071
ΔCCSD(T)	aug-cc-pVDZ	2.5401	0.0322
	d-aug-cc-pVDZ	2.7727	0.0372
	t-aug-cc-pVDZ	2.6694	0.6235
	aug-cc-pVTZ	2.3678	0.3940
	d-aug-cc-pVTZ	2.4952	0.5432
	t-aug-cc-pVTZ	2.4940	0.4426
	aug-cc-pVQZ	2.3284	0.4049
	d-aug-cc-pVQZ	2.4343	0.5048
	t-aug-cc-pVQZ	2.4564	0.4563

TABLE IV. Positions and widths (in eV) of the $^2\Pi_g$, N_2^- shape resonance computed using the type II-Coulomb method. Note that the method does not have the stability of the type III-Coulomb method, but it does provide a more accurate value for the width.

we observe severe numerical problems.

Furthermore, we note that at the ΔSCF level of theory, the results agree well with the complex basis function results of Ref. 51 computed at the same level of theory (see the "NH-UHF" row of Table II). This agreement between different methods at the same approximate level of theory is encouraging. The fact that the CCSD(T) results do not reproduce the accepted value in the largest basis set is not surprising, because even in this basis, the numbers do not appear to be converged with respect to basis set size. It is also possible that the results are not fully converged with these treatments of correlation.

C. Evaluation of the type III-Gaussian method

The type III method with an added Gaussian potential is found to be critically dependent upon the form of the added Gaussian potential. Some results for three different Gaussian exponents are shown in Table V. Note that despite the apparently good basis set convergence for a given value of α, the resonance parameters are very dependent on the exponent of the Gaussian potential. This suggests that the functional form used for the analytic continuation is not sufficiently flexible to accurately model $\lambda(\kappa)$ for all values of α. This is consistent with the performance of the type III methods on the model potential.

Using a higher level of theory and a higher order Padé approximant improves the agreement between the $\alpha = 0.01$ and $\alpha = 0.1$ cases, but does little to improve the $\alpha = 1$ case. This further suggests that the [2/1] Padé approximant is not sufficiently flexible to accurately describe the complex energy as a function of the coupling constant. Also, as noted in Section IV A, the [4/2] Padé approximation is in practical terms much inferior to the simpler [2/1] and [3/1] approximations. The non-linear, least-square optimization is much more difficult to solve and, unlike in the [2/1] case, there can be several nearby minima.

Both the failure of the type III-Gaussian method, and the moderate success of the type III-Coulomb method can be explained by the model potential calculations shown in Figures 2 and 3. These trajectories suggest that the Gaussian potential gives rise to an analytic form that is more complicated than that of the Coulomb potential and is therefore more difficult to reproduce with the simple Padé approximants used in the type III method.

D. Evaluation of the type II-Gaussian method

The type II-Gaussian method uses a functional form that is significantly more flexible than the low order Padé approximations used in the type III family of methods which should, to some extent, remedy the problem discussed in Section IV C. The results for different basis sets at the ΔSCF and ΔCCSD(T) levels of theory are shown in Table VI. Overall, the results are much more consistent as the exponent of the added Gaussian potential is varied. That being said, the numbers are not as stable with respect to basis set size as in the type III method, and there is still an undesirable α-dependence.

For the CCSD(T) results, there is again fairly good agreement when the exponent of the added Gaussian potential is changed over 2 orders of magnitude. There is still disagreement for $\alpha = 1$, but such a narrow Gaussian affects the core orbitals so disproportionately relative to the diffuse orbitals, that a basis set with core-valence polarization functions and/or a higher-level treatment of electron correlation may be necessary to achieve solid agreement in this case.

E. Evaluation of the type III-attenuated Coulomb method

The results of the type III-attenuated Coulomb method applied to the $^2\Pi_g$ shape resonance in N_2 are shown in Table VII at the ΔSCF and ΔCCSD(T) levels of theory. For a small attenuation parameter, there is negligible difference between these results and the results obtained with the Coulomb potential. Despite apparent basis-set convergence, the numbers have an ω-dependence that is nonetheless not as severe as the α-dependence in the case of the Gaussian potential. More distressing is that the widths do not appear to converge to the accepted value of the width. However the position of the resonance seems to be computed accurately and has very little ω-dependence at the CCSD(T) level of theory.

method	basis	$\alpha = 0.01$		$\alpha = 0.1$		$\alpha = 1.00$	
		Position	Width	Position	Width	Position	Width
ΔSCF [2/1]	aug-cc-pVDZ	2.8433	0.0513	2.9523	0.4598	2.5565	2.9050
	d-aug-cc-pVDZ	2.8029	0.0784	2.9448	0.4599	2.6556	2.9297
	t-aug-cc-pVDZ	2.8006	0.0802	2.9449	0.4604	2.5456	2.8870
	aug-cc-pVTZ	2.8215	0.0590	2.9291	0.4606	2.6216	2.7584
	d-aug-cc-pVTZ	2.7972	0.0757	2.9264	0.4662	2.7144	2.7894
	t-aug-cc-pVTZ	2.7970	0.0766	2.9265	0.4679	2.6209	2.7557
	aug-cc-pVQZ	2.6237	0.0608	2.9250	0.4686	2.6996	2.7860
	d-aug-cc-pVQZ	2.7977	0.0761	2.9248	0.4701	2.6024	2.7506
	t-aug-cc-pVQZ	2.7976	0.0761	2.9251	0.4705	2.5600	2.7328
ΔCCSD(T) [2/1]	t-aug-cc-pVQZ	2.2089	0.1707	2.5551	0.5163	2.4757	2.9159
ΔCCSD(T), [4/2]	t-aug-cc-pVQZ	2.4018	0.6343	2.5317	0.5752	2.5608	2.4871

TABLE V. Positions and widths (in eV) of the $^2\Pi_g$, N_2^- shape resonance computed using the type III-Gaussian method at the ΔSCF and ΔCCSD(T) levels of theory. Note the strong dependence on the exponent of the added Gaussian potential (α).

method	basis	$\alpha = 0.01$		$\alpha = 0.1$		$\alpha = 1.00$	
		Position	Width	Position	Width	Position	Width
ΔSCF	aug-cc-pVDZ	2.8423	-0.0008	2.8394	0.0415	2.8129	0.4298
	d-aug-cc-pVDZ	2.8875	0.0871	2.8515	0.1599	2.8006	0.4190
	t-aug-cc-pVDZ	2.8327	0.2327	2.8491	0.1721	2.8307	0.2376
	aug-cc-pVTZ	2.8064	0.0015	2.7958	0.0671	2.8533	0.3916
	d-aug-cc-pVTZ	2.8512	0.1279	2.8377	0.1553	2.8081	0.4032
	t-aug-cc-pVTZ	2.8358	0.2158	2.8415	0.1673	2.7915	0.3429
	aug-cc-pVQZ	2.5834	0.0034	2.8039	0.1559	2.7885	0.3914
	d-aug-cc-pVQZ	2.8326	0.2005	2.8380	0.1742	2.8452	0.4210
	t-aug-cc-pVQZ	2.8299	0.2154	2.8412	0.1718	2.7963	0.4007
ΔCCSD(T)	t-aug-cc-pVQZ	2.4419	0.5908	2.4820	0.5360	2.4510	0.7185

TABLE VI. Positions and widths (in eV) of the $^2\Pi_g$, N_2^- shape resonance computed using the type II-Gaussian method. Note that there is significantly reduced dependence on the exponent of the added Gaussian potential (α).

method	basis	$\omega = 0.001$		$\omega = 0.01$		$\omega = 0.1$	
		Position	Width	Position	Width	Position	Width
ΔSCF [2/1]	aug-cc-pVDZ	2.74217	0.70854	2.75251	0.72708	2.68530	1.05547
	d-aug-cc-pVDZ	2.73879	0.70692	2.74905	0.72543	2.75149	1.02148
	t-aug-cc-pVDZ	2.73920	0.70719	2.74781	0.72579	2.75192	1.02192
	aug-cc-pVTZ	2.76522	0.62485	2.77457	0.64119	2.72995	0.93501
	d-aug-cc-pVTZ	2.76209	0.62746	2.77149	0.64389	2.73919	0.92092
	t-aug-cc-pVTZ	2.76227	0.62849	2.77171	0.64494	2.73911	0.92266
	aug-cc-pVQZ	2.76087	0.63085	2.77034	0.64736	2.72381	0.94495
	d-aug-cc-pVQZ	2.75966	0.63175	2.76914	0.64830	2.73459	0.92812
	t-aug-cc-pVQZ	2.75972	0.63200	2.76921	0.64855	2.73479	0.92839
ΔCCSD(T) [2/1]	aug-cc-pVDZ	2.55822	0.77198	2.57251	0.79356	2.56588	1.14238
	d-aug-cc-pVDZ	2.49861	0.78082	2.50061	0.80643	2.54943	1.13871
	t-aug-cc-pVDZ	2.51745	0.77596	2.49981	0.80661	2.54894	1.13888
	aug-cc-pVTZ	2.41852	0.61804	2.42736	0.63629	2.47546	0.89812
	d-aug-cc-pVTZ	2.38092	0.62691	2.38958	0.64573	2.45552	0.90377
	t-aug-cc-pVTZ	2.37963	0.62805	2.38836	0.64690	2.45512	0.90525
	aug-cc-pVQZ	2.35958	0.60802	2.36776	0.62623	2.37978	0.89098
	d-aug-cc-pVQZ	2.33540	0.61272	2.34348	0.63124	2.37299	0.89164
	t-aug-cc-pVQZ	2.33466	0.61301	2.34256	0.63159	2.39789	0.88717

TABLE VII. Positions and widths (in eV) of the $^2\Pi_g$, N_2^- shape resonance computed using the type III-attenuated Coulomb method with a [2/1] Padé approximant at various levels of theory. Note the dependence on the attenuation parameter (ω).

	Position	Width
ΔSCF	2.76921	0.64855
ΔMP2	2.54952	0.68410
ΔCCSD	2.34915	0.61525
ΔCCSD(T)	2.34256	0.63159

TABLE VIII. Positions and widths (in eV) of the $^2\Pi_g$, N_2^- shape resonance computed using the type III-attenuated Coulomb method using a [2/1] Padé approximant at various levels of theory. The basis set is the t-aug-cc-pVQZ basis set and $\omega = 0.01$.

For completeness, the results in the largest basis set using a [4/2] Padé approximant are given in the supplementary material (Table VII). Only for $\omega = 0.1$ was the [4/2] fit different than the [2/1] at the ΔSCF level of theory. Despite this very slight improvement in the ω-dependence, the results are not significantly different, and again fitting the the [4/2] Padé approximant proved to be a more difficult optimization problem.

Some results for different treatments of correlation in the largest basis set are shown in Table VIII. As we might expect, MP2 theory recovers a significant, but still incomplete, portion of the correlation contribution. The effect of the triples correction is negligible in this case. The width does not change significantly as the treatment or correlation is changed, and it does not converge to the accepted value.

F. Evaluation of the type II-attenuated Coulomb method

The type II-attenuated Coulomb method performs well when applied to the $^2\Pi_g$, N_2^- shape-resonance. The results at the ΔSCF and ΔCCSD(T) levels of theory are shown in Table IX. Despite slow convergence with respect to the diffuse part of the basis set, the type II-attenuated Coulomb method has negligible ω-dependence. In the largest basis, the results do not quite converge to the accepted value, but it is apparent the the numbers are not entirely converged with respect to the basis set. At the ΔSCF level of theory, the results agree remarkably well with the complex basis function, non-Hermitian UHF results of Ref. 51. Finally, notice that the dependence on ω is small compared to probable error due to the incomplete basis and incomplete description of electron correlation. The primary drawback of this method that it requires a large, diffuse basis set to achieve consistent results.

Results for different treatments of electron correlation are shown in Table X. Both the position and the width are significantly affected by the level of correlation in a manner which is consistent with other methods. The results at the CCSD level of theory agree fairly well with the EOM-EA-CCSD stabilization results presented in Ref. 49. The small differences are easily attributed to the slightly different level of theory and the different basis set.

V. CONCLUSIONS AND FUTURE WORK

The performance of two different analytic continuation schemes for 3 classes of stabilizing potentials has been critically evaluated. Results for a model problem suggest that the accuracy of the type III methods is limited by the simple functional form. Furthermore, the results for both analytic continuation schemes depend on the functional form of the stabilizing potential. While the Gaussian potential is short-range, better results are obtained with the Coulomb potential. An attenuated Coulomb potential retains the best features of the Coulomb potential without the long range tail. It is with the attenuated Coulomb potential that the best results are obtained.

The performance of the type III method on the $^2\Pi_g$ state of N_2^- is surprisingly good. There is systematic error in the width, but the position agrees well with the accepted value. The type III-Gaussian method does not perform well; this is probably due to a lack of flexibility in the functional form used in the analytic continuation. We do not recommend the use of a Gaussian potential. The type III-attenuated Coulomb method is somewhat sensitive to the attenuation parameter, ω, but retains many of the nice features of the type III-Coulomb method while being formally justifiable. We recommend an ω-value lying in the range that we have investigated (0.001-0.1). This broad range of ω, corresponding to characteristic lengths in the range 10 to 1000 Bohr, is likely appropriate for most low energy shape resonances which share physical characteristics with the N_2^- shape resonance.

The type II method performs decently well for all three potentials, though both the accuracy and basis-set convergence properties are best when combined with the attenuated Coulomb potential. Despite slow basis set convergence and some sensitivity to the precision of the inputs, in no case did we observe multiple nearby solutions or other pathological numerical problems. Furthermore, analytic continuation with type II Padé approximants provided more accurate widths, significantly less ω-dependence, and agreed better with other theoretical methods. We therefore suggest that the use of such high order Padè approximants in the analytic continuation of the inverse problem should not be discounted, especially if high precision input data is available. The type III-Coulomb or type III-attenuated Coulomb method may be used in cases where precise computations in large basis sets are not feasible, but with the caveat that there will likely be systematic error in the computed widths.

To summarize, for the IACCC method:

- We suggest an attenuated Coulomb potential as a formally justifiable, simple to implement alternative to a Coulomb potential.
- The type II method is most accurate and should be used if high precision calculations in large basis

	basis	$\omega = 0.001$		$\omega = 0.01$		$\omega = 0.1$	
		Position	Width	Position	Width	Position	Width
SCF	aug-cc-pVDZ	2.83173	-0.00320	2.83333	0.00155	2.82576	0.01793
	d-aug-cc-pVDZ	2.84264	0.16154	2.84648	0.16814	2.84740	0.16000
	t-aug-cc-pVDZ	2.85043	0.17558	2.84711	0.17931	2.84503	0.18047
	aug-cc-pVTZ	2.79090	0.00204	2.74397	0.10855	2.77907	0.07895
	d-aug-cc-pVTZ	2.83293	0.16192	2.83551	0.15931	2.83411	0.16129
	t-aug-cc-pVTZ	2.79914	0.20080	2.79953	0.17272	2.83240	0.18002
	aug-cc-pVQZ	2.78391	0.22003	2.81807	0.06469	2.77191	0.20154
	d-aug-cc-pVQZ	2.83282	0.18578	2.82263	0.10278	2.83902	0.17423
	t-aug-cc-pVQZ	2.80872	0.20374	2.81202	0.19265	2.83933	0.17521
CCSD(T)	aug-cc-pVDZ	2.72974	0.04936	2.61625	0.01137	2.69380	-0.12249
	d-aug-cc-pVDZ	2.58293	0.58125	2.51936	0.53558	2.68915	0.60403
	t-aug-cc-pVDZ	2.60820	0.54588	2.70268	0.51919	2.66480	0.57979
	aug-cc-pVTZ	2.55929	0.28910	2.38274	-0.16756	2.27533	-0.24968
	d-aug-cc-pVTZ	2.38438	0.02248	2.58832	0.28094	2.50422	0.48415
	t-aug-cc-pVTZ	2.52261	0.52226	2.57618	0.53210	2.50365	0.49965
	aug-cc-pVQZ	2.30677	0.35992	2.45588	0.43936	2.37634	0.49320
	d-aug-cc-pVQZ	2.48175	0.47893	2.48287	0.29264	2.45698	0.46146
	t-aug-cc-pVQZ	2.47390	0.48362	2.46018	0.48523	2.45495	0.46199

TABLE IX. Positions and widths (in eV) of the $^2\Pi_g$, N_2^- shape resonance computed using the type II-attenuated Coulomb method at various levels of theory.

method	Position	Width
ΔSCF	2.81202	0.19265
ΔMP2	2.58212	0.47505
ΔCCSD	2.47772	0.41312
ΔCCSD(T)	2.46018	0.48523

TABLE X. Positions and widths (in eV) of the $^2\Pi_g$, N_2^- shape resonance computed using the type II-attenuated Coulomb method at various levels of theory. The basis set is the t-aug-cc-pVQZ basis set and $\omega = 0.01$.

sets are feasible.

- The type III method can be used in cases where the use of large basis sets is not feasible, but there will likely be systematic error in the computed widths.

SUPPLEMENTARY MATERIAL

See supplementary material for the full set of results for all basis sets and methods

ACKNOWLEDGMENTS

This material is based upon work supported by the U.S. Department of Energy, Office of Science, Office of Advanced Scientific Computing Research, Scientific Discovery through Advanced Computing (SciDAC) program. Work at LBNL was performed under the auspices of the U.S. Department of Energy under Contract DE-AC02-05CH11231.

Appendix A: Derivatives of type III RAC Padé approximants

In order to solve the non-linear least-squares problem, we minimize

$$\chi^2 = \frac{1}{N}\sum_{i=1}^{N}\left|\tilde{\lambda}(\kappa_i) - \lambda_i\right| \tag{A1}$$

where $\tilde{\lambda}(\kappa)$ is one of either $\lambda^{[2/1]}(\kappa;\alpha,\beta,\lambda_0)$, $\lambda^{[3/1]}(\kappa;\alpha,\beta,\delta,\lambda_0)$, or $\lambda^{[4/2]}(\kappa;\alpha,\beta,\gamma,\delta,\epsilon,\lambda_0)$. The non-linear optimization can be easily accomplished using a some variant of Newton's method with analytic derivatives of χ^2 from which finite difference second derivatives can be computed. Specifically, we require derivatives with respect to the fitting parameters α, β, etc. Since all of these Padé approximants have the form

$$\lambda^{[N/M]} = \lambda_0 g^{[N/M]}, \tag{A2}$$

the derivative of χ^2 with respect to λ_0 is trivial, and we further require only the derivatives of $g^{[M/N]}$ with respect to the remaining parameters.

For the [2/1] Padé approximant, we get

$$\frac{\partial g^{[2/1]}}{\partial \alpha} = \frac{4\alpha\kappa + 4\alpha^3}{\alpha^4 + \beta^2 + 2\alpha^2\kappa} - \frac{\kappa^2 + 2\alpha^2\kappa + \alpha^4 + \beta^2}{(\alpha^4 + \beta^2 + 2\alpha^2\kappa)^2}(4\alpha\kappa + 4\alpha^3) \tag{A3}$$

$$\frac{\partial g^{[2/1]}}{\partial \beta} = \frac{2\beta}{\alpha^4 + \beta^2 + 2\alpha^2\kappa} - \frac{\kappa^2 + 2\alpha^2\kappa + \alpha^4 + \beta^2}{(\alpha^4 + \beta^2 + 2\alpha^2\kappa)^2}(2\beta) \tag{A4}$$

For the [3/1] Padé approximant, we get

$$\frac{\partial g^{[3/1]}}{\partial \alpha} = \frac{(4\alpha\kappa + 4\alpha^3)(1+\delta^2\kappa)}{\alpha^4 + \beta^2 + \kappa[2\alpha^2 + \delta^2(\alpha^4+\beta^2)]} - \frac{(\kappa^2 + 2\alpha^2\kappa + \alpha^4 + \beta^2)(1+\delta^2\kappa)}{\{\alpha^4 + \beta^2 + \kappa[2\alpha^2 + \delta^2(\alpha^4+\beta^2)]\}^2}(4\alpha^3 + 4\alpha\kappa + 4\delta^2\alpha^3\kappa) \tag{A5}$$

$$\frac{\partial g^{[3/1]}}{\partial \beta} = \frac{2\beta(1+\delta^2\kappa)}{\alpha^4 + \beta^2 + \kappa[2\alpha^2 + \delta^2(\alpha^4+\beta^2)]} - \frac{(\kappa^2 + 2\alpha^2\kappa + \alpha^4 + \beta^2)(1+\delta^2\kappa)}{\{\alpha^4 + \beta^2 + \kappa[2\alpha^2 + \delta^2(\alpha^4+\beta^2)]\}^2}(2\beta + 2\delta^2\beta\kappa) \tag{A6}$$

$$\frac{\partial g^{[3/1]}}{\partial \delta} = \frac{(\kappa^2 + 2\alpha^2\kappa + \alpha^4 + \beta^2)2\delta\kappa}{\alpha^4 + \beta^2 + \kappa[2\alpha^2 + \delta^2(\alpha^4+\beta^2)]} - \frac{(\kappa^2 + 2\alpha^2\kappa + \alpha^4 + \beta^2)(1+\delta^2\kappa)}{\{\alpha^4 + \beta^2 + \kappa[2\alpha^2 + \delta^2(\alpha^4+\beta^2)]\}^2}2\delta(\alpha^4+\beta^2)\kappa \tag{A7}$$

For the [4/2] Padé approximate, we define the numerator and denominator as

$$N \equiv (\kappa^2 + 2\alpha^2\kappa + \alpha^4 + \beta^2)(\kappa^2 + 2\gamma^2\kappa + \gamma^4 + \delta^2) \qquad D \equiv (\alpha^4+\beta^2)(\gamma^4+\delta^2)(1+\mu^2\kappa)(1+\mu^2\epsilon^2\kappa), \tag{A8}$$

as well as the derivatives of μ^2:

$$\mu_\alpha^2 \equiv \frac{\partial \mu^2}{\partial \alpha} = \frac{2}{\epsilon^2+1}\left[\frac{2\alpha}{\alpha^4+\beta^2} - \frac{4\alpha^5}{(\alpha^4+\beta^2)^2}\right] \qquad \mu_\beta^2 \equiv \frac{\partial \mu^2}{\partial \beta} = -\frac{4\alpha^2\beta}{(\epsilon^2+1)(\alpha^4+\beta^2)} \tag{A9}$$

$$\mu_\gamma^2 \equiv \frac{\partial \mu^2}{\partial \gamma} = \frac{2}{\epsilon^2+1}\left[\frac{2\gamma}{\gamma^4+\delta^2} - \frac{4\gamma^5}{(\gamma^4+\delta^2)^2}\right] \qquad \mu_\delta^2 \equiv \frac{\partial \mu^2}{\partial \delta} = -\frac{4\gamma^2\delta}{(\epsilon^2+1)(\gamma^4+\delta^2)} \tag{A10}$$

$$\mu_\epsilon^2 \equiv \frac{\partial \mu^2}{\partial \epsilon} = -\frac{4\epsilon}{(\epsilon^2+1)^2}\left[\frac{\alpha^2}{\alpha^4+\beta^2} + \frac{\gamma^2}{\gamma^4+\delta^2}\right]. \tag{A11}$$

In terms of these quantities, the derivatives are given by

$$\frac{\partial g^{[4/2]}}{\partial \alpha} = \frac{4(\alpha\kappa+\alpha^3)(\kappa^2+2\gamma^2\kappa+\gamma^4+\delta^2)}{D} - \frac{4N\alpha^3}{(\alpha^4+\beta^2)D} - \frac{N\mu_\alpha^2\kappa}{(1+\mu^2\kappa)D} - \frac{N\epsilon^2\mu_\alpha^2\kappa}{(1+\mu^2\epsilon^2\kappa)D} \tag{A12}$$

$$\frac{\partial g^{[4/2]}}{\partial \beta} = \frac{(2\beta)(\kappa^2+2\gamma^2\kappa+\gamma^4+\delta^2)}{D} - \frac{2N\beta}{(\alpha^4+\beta^2)D} - \frac{N\mu_\beta^2\kappa}{(1+\mu^2\kappa)D} - \frac{N\epsilon^2\mu_\beta^2\kappa}{(1+\mu^2\epsilon^2\kappa)D} \tag{A13}$$

$$\frac{\partial g^{[4/2]}}{\partial \gamma} = \frac{(\kappa^2+2\alpha^2\kappa+\alpha^4+\beta^2)4(\gamma\kappa+\gamma^3)}{D} - \frac{4N\gamma^3}{(\gamma^4+\delta^2)D} - \frac{N\mu_\gamma^2\kappa}{(1+\mu^2\kappa)D} - \frac{N\epsilon^2\mu_\gamma^2\kappa}{(1+\mu^2\epsilon^2\kappa)D} \tag{A14}$$

$$\frac{\partial g^{[4/2]}}{\partial \delta} = \frac{(\kappa^2+2\alpha^2\kappa+\alpha^4+\beta^2)(2\delta)}{D} - \frac{2N\delta}{(\gamma^4+\delta^2)D} - \frac{N\mu_\delta^2\kappa}{(1+\mu^2\kappa)D} - \frac{N\epsilon^2\mu_\delta^2\kappa}{(1+\mu^2\epsilon^2\kappa)D} \tag{A15}$$

$$\frac{\partial g^{[4/2]}}{\partial \epsilon} = -N\left[\frac{\mu_\epsilon^2\kappa}{(1+\mu^2\kappa)D} + \frac{\mu_{\epsilon^2}\epsilon^2\kappa + 2\epsilon\mu^2\kappa}{(1+\mu^2\epsilon^2\kappa)D}\right] \tag{A16}$$

Appendix B: Molecular Gaussian attraction integrals

The analytic continuation methods involving an added Gaussian potential require integrals of the form

$$\langle\phi_\mu|U_G|\phi_\nu\rangle = -\sum_{k=1}^{P} A_k V_{\mu\nu}^{(k)} \tag{B1}$$

where

$$V_{\mu\nu}^{(k)} \equiv \int d^3\mathbf{r}\phi_\mu(\mathbf{r})e^{-\alpha(\mathbf{r}-\mathbf{C}_k)^2}\phi_\nu(\mathbf{r}). \tag{B2}$$

The sum over k is over Gaussian potentials centered at $\mathbf{C}_k$ and ϕ_μ, ϕ_ν are primitive Gaussian type orbitals. In order to derive an explicit formula for these integrals, we first use Gaussian product theorem (GPT) twice to combine the three Gaussian factors into a single Gaussian:

$$N_\mu N_\nu G_{AB} G_{PC} P(x,y,z)\exp\left[-\eta(\mathbf{r}-\mathbf{Q})\right]. \tag{B3}$$

The polynomial, $P(x,y,z)$ is just a product of polynomial factors from the two basis functions, N_μ and N_ν are normalization factors, and the other quantities are given

by

$$G_{\mathbf{PC}} = \exp\left[-\frac{\gamma\alpha}{\gamma+\alpha}(\mathbf{P}-\mathbf{C})^2\right]$$
$$\eta = \gamma + \alpha$$
$$\mathbf{Q} = \frac{\gamma\mathbf{P}+\alpha\mathbf{C}}{\gamma+\alpha} \tag{B4}$$

where $\mathbf{P}$ and γ are the GPT center and exponent associated with the product of basis functions. The explicit formula is now easily derived in analogy to the case of simple overlap integrals given in Ref. 55. This allows for direct reuse of the explicit formulas that are used to compute overlaps, the only difference is that $\mathbf{P} \to \mathbf{Q}$ and $\gamma \to \eta$. We compute the integrals using this method. However it is also possible to compute the integrals using a special case of the recurrence relation for 3-center overlaps given by Obara and Saika:[56]

$$(\mathbf{a}+\mathbf{1}_i|\mathbf{0}|\mathbf{b}) = \frac{a_i}{2\eta}(\mathbf{a}-\mathbf{1}_i|\mathbf{0}|\mathbf{b}) + \frac{b_i}{2\eta}(\mathbf{a}|\mathbf{0}|\mathbf{b}-\mathbf{1}_i) + (Q_i - A_i)(\mathbf{a}|\mathbf{0}|\mathbf{b}). \tag{B5}$$

The extension of either method to contracted Gaussian basis functions is trivial.

[1] J. Taylor, Scattering Theory (John Wiley {&} Sons, Inc., New York, 1972).
[2] K. D. Jordan, V. K. Voora, and J. Simons, Theor. Chem. Acc. **133**, 1 (2014).
[3] V. I. Kukulin, V. M. Krasnopolsky, and J. Horcek, Theory of Resonances: Principles and Applications (Kluwer Academic, 1989).
[4] N. Moiseyev, Phys. Rep. **302**, 211 (1998).
[5] B. Schneider, Chem. Phys. Lett. **31**, 237 (1975).
[6] R. R. Lucchese, D. Watson, and V. McKoy, Phys. Rev. A **22**, 421 (1980).
[7] B. I. Schneider and T. N. Rescigno, Phys. Rev. A **37**, 3749 (1988).
[8] W. M. Huo and F. A. Gianturco, eds., Computational Methods for Electron-Molecule Collisions (Springer, New York, 1993).
[9] J. Tennyson, Phys. Rep. **491**, 29 (2010).
[10] R. F. da Costa, M. T. D. N. Varella, M. H. F. Bettega, and M. a. P. Lima, The European Physical Journal D **69**, 159 (2015).
[11] H. S. Taylor, Adv. Chem. Phys. **18**, 91 (1970).
[12] A. U. Hazi and H. S. Taylor, Phys. Rev. A **1**, 1109 (1970).
[13] J. Simons, J. Chem. Phys. **75**, 2465 (1981).
[14] C. W. McCurdy and J. McNutt, Chem. Phys. Lett. **94**, 306 (1983).
[15] R. Frey and J. Simons, J. Chem. Phys. **84**, 4462 (1986).
[16] P. Winkler, Zeitschrift für Physik A Atoms and Nuclei **160**, 149 (1977).
[17] C. McCurdy and T. Rescigno, Phys. Rev. Lett. **41**, 1364 (1978).
[18] W. Reinhardt, Annu. Rev. Phys. Chem. **33**, 223 (1982).
[19] U. Riss and H. Meyer, J. Phys. B: At., Mol. Opt. Phys. **26**, 4503 (1993).
[20] T. Jagau, D. Zuev, K. B. Bravaya, E. Epifanovsky, and A. I. Krylov, J. Phys. Chem. Lett. **5**, 310 (2013).
[21] A. F. White, M. Head-Gordon, and C. W. McCurdy, J. Chem. Phys. **142**, 054103 (2015).
[22] B. Nestmann and S. D. Peyerimhoff, J. Phys. B: At. Mol. Phys. **18**, 615 (1985).
[23] B. M. Nestmann and S. D. Peyerimhoff, J. Phys. B: At. Mol. Phys. **18**, 4309 (1985).
[24] V. Kukulin and V. Krasnopolsky, J. Phys. A: Gen. Phys. **10**, 32 (1977).
[25] J. Horáček, P. Mach, and J. Urban, Phys. Rev. A **82**, 032713 (2010).
[26] V. Krasnopolsky and V. Kukulin, Physics Letters **69**, 251 (1978).
[27] P. Papp, Š. Matejčík, P. Mach, J. Urban, I. Paidarová, and J. Horáček, Chem. Phys. **418**, 8 (2013).
[28] T. Sommerfeld and M. Ehara, J. Chem. Phys. **142**, 034105 (2015).
[29] J. Horáček, I. Paidarová, and R. Čurík, J. Chem. Phys. **143**, 184102 (2015).
[30] R. Čurík, I. Paidarová, and J. Horáček, Euro. Phys. J. D. **70**, 146 (2016).
[31] D. Bessis, J. Comput. Appl. Math. **66**, 85 (1996).
[32] G. A. Baker and P. Graves-Morris, Padé Approximants (Cambridge University Press, 1996).
[33] J. Horáček, I. Paidarová, and R. Curik, J. Phys. Chem. A **118**, 6536 (2014).
[34] L. Schlessinger, Phys. Rev. **36**, 1411 (1968).
[35] R. Adamson, J. Dombroski, and P. Gill, J. Comput. Chem. **20**, 921 (1999).
[36] N. A. Besley, M. J. G. Peach, and D. J. Tozer, Phys. Chem. Chem. Phys. **11**, 10350 (2009).
[37] L. Tao, C. W. McCurdy, and T. N. Rescigno, Physical Review A - Atomic, Molecular, and Optical Physics **79**, 1 (2009).
[38] L. Tao, C. W. McCurdy, and T. N. Rescigno, Physical Review A - Atomic, Molecular, and Optical Physics **80**, 1 (2009).
[39] L. Tao, C. W. McCurdy, and T. N. Rescigno, Physical Review A - Atomic, Molecular, and Optical Physics **82**, 1 (2010).
[40] S. L. Guberman and A. Giusti-Suzor, J. Chem. Phys. **95**, 2602 (1991).
[41] W. H. Miller and H. Morgner, J. Chem. Phys. **67**, 4923 (1977).
[42] I. Sánchez and F. Martín, J. Chem. Phys. **106**, 7720 (1997).
[43] F. Morales, C. W. McCurdy, and F. Martín, Phys. Rev. A **73**, 014702 (2006).
[44] W. Domcke, J. Phys. B: At. Mol. Phys. **16**, 359 (1983).
[45] Y. Shao, Z. Gan, E. Epifanovsky, A. T. Gilbert, M. Wormit, J. Kussmann, A. W. Lange, A. Behn, J. Deng, X. Feng, D. Ghosh, M. Goldey, P. R. Horn, L. D. Jacobson, I. Kaliman, R. Z. Khaliullin, T. Kuś, A. Landau, J. Liu, E. I. Proynov, Y. M. Rhee, R. M. Richard, M. a. Rohrdanz, R. P. Steele, E. J. Sundstrom, H. L. Woodcock, P. M. Zimmerman, D. Zuev, B. Albrecht, E. Alguire, B. Austin, G. J. O. Beran, Y. a. Bernard, E. Berquist, K. Brandhorst, K. B. Bravaya, S. T. Brown, D. Casanova, C.-M. Chang, Y. Chen, S. H. Chien, K. D. Closser, D. L. Crittenden, M. Diedenhofen, R. a. DiStasio, H. Do, A. D. Dutoi, R. G. Edgar, S. Fatehi, L. Fusti-Molnar, A. Ghysels, A. Golubeva-Zadorozhnaya, J. Gomes, M. W. Hanson-Heine, P. H. Harbach, A. W. Hauser, E. G. Hohenstein, Z. C. Holden, T.-C. Jagau, H. Ji, B. Kaduk, K. Khistyaev, J. Kim, J. Kim, R. a. King, P. Klunzinger, D. Kosenkov, T. Kowalczyk, C. M. Krauter, K. U. Lao, A. Laurent, K. V. Lawler, S. V. Levchenko, C. Y. Lin, F. Liu, E. Livshits, R. C. Lochan, A. Luenser, P. Manohar, S. F. Manzer, S.-P. Mao, N. Mardirossian, A. V. Marenich, S. a. Maurer, N. J. Mayhall, E. Neuscamman, C. M. Oana, R. Olivares-Amaya, D. P. O'Neill, J. a. Parkhill, T. M. Perrine, R. Peverati, A. Prociuk, D. R. Rehn, E. Rosta, N. J. Russ, S. M. Sharada, S. Sharma, D. W. Small, A. Sodt, T. Stein, D. Stück, Y.-C. Su, A. J. Thom, T. Tsuchimochi, V. Vanovschi, L. Vogt, O. Vydrov, T. Wang, M. a. Watson, J. Wenzel, A. White, C. F. Williams, J. Yang, S. Yeganeh, S. R. Yost, Z.-Q. You, I. Y. Zhang, X. Zhang, Y. Zhao, B. R. Brooks, G. K. Chan, D. M. Chipman, C. J. Cramer, W. a. Goddard, M. S. Gordon, W. J. Hehre, A. Klamt, H. F. Schaefer, M. W. Schmidt, C. D. Sherrill, D. G. Truhlar, A. Warshel, X. Xu, A. Aspuru-Guzik, R. Baer, A. T. Bell, N. a. Besley, J.-D. Chai, A. Dreuw, B. D. Dunietz, T. R. Furlani, S. R. Gwaltney, C.-P. Hsu, Y. Jung, J. Kong, D. S. Lambrecht, W. Liang, C. Ochsenfeld, V. a. Rassolov, L. V. Slipchenko, J. E. Subotnik, T. Van Voorhis, J. M. Herbert, A. I. Krylov, P. M. Gill, and M. Head-Gordon, Mol. Phys. **113**, 184 (2014).

[46]a. Hazi, T. Rescigno, and M. Kurilla, Phys. Rev. A **23**, 1089 (1981).
[47]H.-D. Meyer, Phys. Rev. A **40**, 5605 (1989).
[48]S. Mahalakshmi, A. Venkatnathan, and M. K. Mishra, J. Chem. Phys. **115**, 4549 (2001).
[49]M. F. Falcetta, L. A. Difalco, D. S. Ackerman, J. C. Barlow, and K. D. Jordan, J. Phys. Chem. A **118**, 7489 (2014).
[50]D. Zuev, T.-C. Jagau, K. B. Bravaya, E. Epifanovsky, Y. Shao, E. Sundstrom, M. Head-Gordon, and A. I. Krylov, J. Chem. Phys. **141**, 024102 (2014).
[51]A. F. White, C. W. McCurdy, and M. Head-Gordon, J. Chem. Phys. **143**, 074103 (2015).
[52]M. Berman, H. Estrada, L. S. Cederbaum, and W. Domcke, Phys. Rev. A **28**, 1363 (1983).
[53]T. H. Dunning, J. Chem. Phys. **90**, 1007 (1989).
[54]D. E. Woon and T. H. Dunning, J. Chem. Phys. **100**, 2975 (1994).
[55]H. Taketa, S. Huzinga, and K. O-Ohata, J. Phys. Soc. Jpn. **21**, 2313 (1966).
[56]S. Obara and A. Saika, J. Chem. Phys. **84**, 3963 (1986).